

Structural Divergence in the Products of the Reaction of $[\text{MoCl}(\eta^3\text{-C}_3\text{H}_5)(\text{CO})_2(\text{dmpm})]$ with Nucleophiles

Julio Pérez,^{*,†} Víctor Riera,[†] Amor Rodríguez,[†] Ramón López,[‡] Tomás L. Sordo,[‡] Santiago García-Granda,[‡] Esther García-Rodríguez,[‡] and Agustín Galindo[§]

Departamento de Química Orgánica e Inorgánica-IUQOEM and Departamento de Química Física y Analítica, Facultad de Química, Universidad de Oviedo-CSIC, Oviedo, Spain, and Departamento de Química Inorgánica, Facultad de Química, Universidad de Sevilla, Sevilla, Spain

Received November 5, 2002

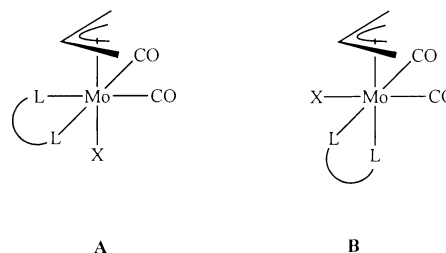
The complex $[\text{MoCl}(\eta^3\text{-allyl})(\text{CO})_2(\text{dmpm})]$ (dmpm = bis(dimethylphosphino)methane) (**1**) reacts with sodium azide and with sodium cyanide to afford the new complexes $[\text{Mo}(\text{N}_3)(\eta^3\text{-allyl})(\text{CO})_2(\text{dmpm})]$ (**2**) and $[\text{Mo}(\text{CN})(\eta^3\text{-allyl})(\text{CO})_2(\text{dmpm})]$ (**3**), respectively, which were characterized spectroscopically and by X-ray diffraction. Complex **2** is a *cis*-dicarbonyl in which one of the P atoms of dmpm is approximately *trans* to a carbonyl, and the other is *trans* to the allyl. In contrast, **3** is a rare *trans*-dicarbonyl. A theoretical analysis was applied to rationalize this difference.

Introduction

The reaction of $[\text{MoX}(\eta^3\text{-allyl})(\text{CO})_2(\text{L-L})]$ (X = anionic monodentate ligand, L-L = neutral diimine or diphosphine chelate) complexes with resonance-stabilized carbanions inspired the use of Mo complexes as allylic alkylation catalysts¹ and models a proposed step of this catalytic process.^{1,2} There are important differences between the complexes with L-L = bipy or phen and those in which L-L is a chelating diphosphine.³ Thus, whereas the former are rigid molecules with the allyl and X occupying mutually *trans* positions (structure A in Chart 1), the latter are fluxional in solution and feature solid state structures with one of the phosphorus donors *trans* to the allyl ligand (structure B in Chart 1).⁴

We have recently isolated stable alkyls and alkynyls $[\text{MoR}(\eta^3\text{-allyl})(\text{CO})_2(\text{N-N})]$ (N-N = 2,2'-bipyridine or 1,10-phenanthroline) from the reaction of chloro precursors with nonstabilized carbanions.⁵ These products retain the above-mentioned features of the halo precursors, i.e., rigidity in solution and a geometry with mutually *trans* R and allyl groups. As a consequence, these alkyl complexes do not undergo reductive elimination of alkyl-allyl coupling products. In contrast, we

Chart 1



found that $[\text{MoCl}(\eta^3\text{-allyl})(\text{CO})_2(\text{dmpm})]$ (dmpm = bis(dimethylphosphino)methane) reacts with acetylide, enolate, or alkyl anions R^- to afford the products of the allyl-anion coupling through the intermediacy of complexes having the R and allyl groups in *cis* positions.⁶ In a first step, the R carbanion substitutes the Cl ligand with a retention of the geometry, and, subsequently, the product isomerizes to an unprecedented *trans*-dicarbonyl complex, which is the species that undergoes the elimination of the R-allyl coupling product.

These results and the lack of previous studies in this area led us to investigate the reactivity of $[\text{MoCl}(\eta^3\text{-allyl})(\text{CO})_2(\text{dmpm})]$ (**1**) with different anions; our first results are the matter of this paper.

Results and Discussion

The reaction of **1** with sodium azide afforded $[\text{Mo}(\text{N}_3)(\eta^3\text{-C}_3\text{H}_5)(\text{CO})_2(\text{dmpm})]$ (**2**). The IR spectrum of **2** showed two intense C–O bands at 1936 and 1851 cm^{-1} , corresponding to the *cis*-Mo(CO)₂ unit, and a strong band at 2072 cm^{-1} , assigned to the azido group. The three-signal pattern for the allyl ligand in ¹H NMR, along with the single peak in ³¹P NMR, is consistent with fluxional behavior, as is typical of $[\text{MoX}(\eta^3\text{-allyl})(\text{CO})_2(\text{P-P})]$ species (see above), given that the molecule of **2** lacks

(6) Pérez, J.; Riera, V.; Rodríguez, A.; García-Granda, S. *Angew. Chem., Int. Ed.* **2002**, *41*, 1427.

* Corresponding author. E-mail: japm@sauron.quimica.uniovi.es.

[†] Departamento de Química Orgánica e Inorgánica-IUQOEM, Universidad de Oviedo-CSIC.

[‡] Departamento de Química Física y Analítica, Universidad de Oviedo.

[§] Universidad de Sevilla.

(1) Trost, B. M.; Lautens, M. *J. Am. Chem. Soc.* **1982**, *104*, 5543.

(2) (a) Trost, B. M.; Merlic, C. A. *J. Am. Chem. Soc.* **1990**, *112*, 9591.

(b) Sjögren, M. P. T.; Frisell, H.; Åkermark, B.; Norrby, P. D.; Eriksson, L.; Vitagliano, A. *Organometallics* **1997**, *16*, 942.

(3) Baker, P. K. *Adv. Organomet. Chem.* **1996**, *40*, 46.

(4) (a) Brisdon, B. J. *J. Organomet. Chem.* **1977**, *125*, 225. (b) Faller, J. W.; Haitko, D. A.; Adams, R. D.; Chodosh, D. F. *J. Am. Chem. Soc.* **1979**, *101*, 865. For exceptions to this trend see ref 2b.

(5) (a) Pérez, J.; Riera, L.; Riera, V.; García-Granda, S.; García-Rodríguez, E. *J. Am. Chem. Soc.* **2001**, *123*, 7469. (b) Pérez, J.; Riera, L.; Riera, V.; García-Granda, S.; García-Rodríguez, E.; Miguel, D. *Organometallics* **2002**, *21*, 1622.

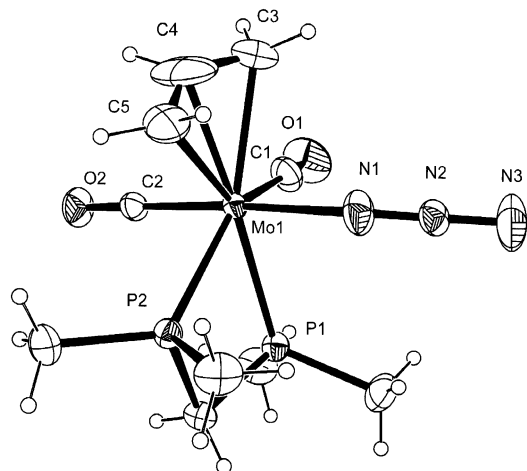


Figure 1. Thermal ellipsoid (30%) plot of complex **2**. Selected bond lengths (Å) and angles (deg): Mo(1)–N(1) 2.270(4), Mo(1)–P(1) 2.4702(12), Mo(1)–P(2) 2.4795(10), N(1)–N(2) 1.128(5), N(2)–N(3) 1.156(5), C(2)–Mo(1)–N(1) 175.14(15), C(1)–Mo(1)–N(1) 101.22(17), N(2)–N(1)–Mo(1) 135.4(3), N(1)–N(2)–N(3) 176.8(5).

any elements of symmetry, as shown by the results of an X-ray structural determination (Figure 1).

The molecule of **2** shows the geometry typically found for $[\text{MoX}(\eta^3\text{-allyl})(\text{CO})_2(\text{P-P})]$ complexes, i.e., P atoms *trans* to the allyl group and to one CO. However, the allyl group of **2** is oriented *endo*, with the open face opposed to the carbonyls.⁷ The normal (*exo*) allyl orientation, with the allyl open face pointing toward the carbonyls, was found in the $[\text{MoX}(\eta^3\text{-allyl})(\text{CO})_2(\text{L-L})]$ compounds that have been structurally characterized so far and was found to be favored for these pseudo-octahedral compounds on the basis of EHMO calculations.⁸ On the other hand, the *endo* orientation, as in **2**, has been found only in complexes with cyclopentadienyl⁹ or tris(pyrazolyl)borato¹⁰ (Tp) ligands occupying the coordination positions of X and dmpm ligands in our complexes.

Compound **1** reacted with NaCN to give $[\text{Mo}(\text{CN})(\eta^3\text{-C}_3\text{H}_5)(\text{CO})_2(\text{dmpm})]$ (**3**). The most striking structural feature of **3** is the mutually *trans* disposition of the two CO ligands, indicated by a single ν_{CO} band at 1867 cm^{-1} and by the two ^{13}C NMR carbonyl signals (a single ν_{CO} band could also be consistent with the presence of a single CO ligand). A weak IR band at 2069 cm^{-1} was assigned to the ν_{CN} stretch of the cyanide ligand. Unlike previously known $[\text{MoX}(\eta^3\text{-allyl})(\text{CO})_2(\text{P-P})]$ compounds, **3** is stereochemically rigid in solution at room temperature, and the structure deduced from the spectroscopic data in solution coincides with that present in the solid state, which was determined by X-ray diffraction (Figure 2). Thus, the OC–Mo–CO angle is $174.1(3)^\circ$. A *trans* M(CO)₂ arrangement in dicarbonyl complexes is electronically disfavored because competition for the back-donation of the metal electron density is maximized between mutually *trans* ligands; hence, strongly π -ac-

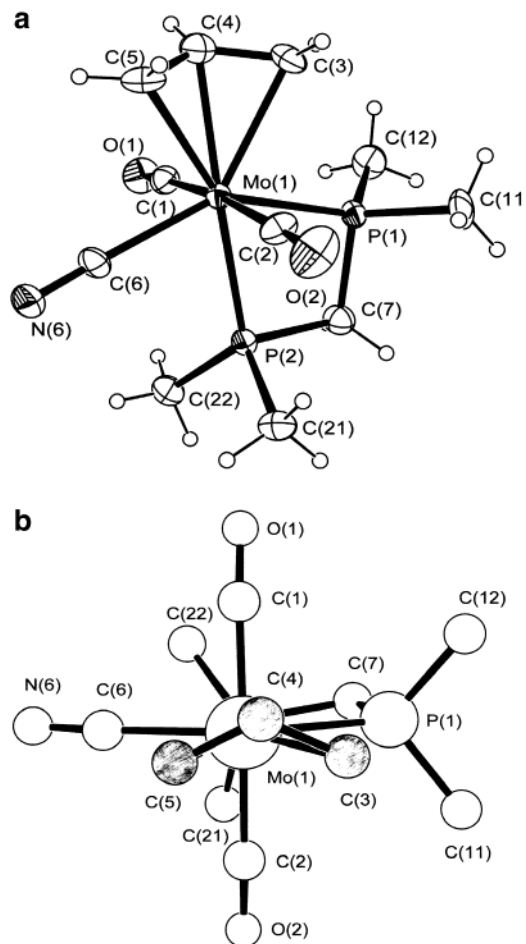


Figure 2. Thermal ellipsoid (30%) plot of complex **3**. Selected bond lengths (Å) and angles (deg): Mo(1)–C(6) 2.255(9), Mo(1)–P(2) 2.501(3), Mo(1)–P(1) 2.504(2), C(6)–N(6) 1.172(11), N(6)–C(6)–Mo(1) 176.5(8).

ceptor CO ligands prefer to be *trans* to ligands other than CO.¹¹ As a result, *trans*-dicarbonyls are very rare and, among the plethora of Mo(II) complexes, virtually unprecedented. Considering together the structures of **2** and **3**, it seems that the *trans* geometry of **3** is due to the electronic properties of the CN ligand (a cyanocomplex isostructural with **2** would not present additional steric hindrance compared with these compounds). It is noteworthy that some of the few other *trans*-dicarbonyl complexes also possess cyano ligands.¹²

Also remarkable is that, whereas malonate-type anions attack the allyl group of $[\text{MoX}(\eta^3\text{-allyl})(\text{CO})_2(\text{L-L})]$ complexes,^{1,13} the reactions of **1** with azide and with cyanide give a single product resulting from chloride substitution in each case, which, despite the mutually *cis* disposition of the $\eta^3\text{-C}_3\text{H}_5$ group and the ligand resulting from the incoming nucleophile, does not undergo coupling.

The orientation of the allyl ligand in **3**, displayed in Figure 2b,¹⁴ deprives the molecule of **3** of a mirror plane,

(7) Curtis, M. D.; Eisenstein, O. *Organometallics* **1984**, *3*, 887.

(8) The angle between the vectors (centroid of Mo(CO)₂–Mo) and allyl central carbon–(centroid of the allyl) have been used to specify the rotational orientation of η^3 -allyl ligands.⁹ These angles are $41(1)^\circ$ and $19.7(5)^\circ$ for **2** and **3**, respectively.

(9) Faller, J. W.; Linebarrier, D. *Organometallics* **1988**, *7*, 1670.

(10) Frohnapfel, D. S.; White, P. S.; Templeton, J. L.; Rügger, H.; Pregosin, P. S. *Organometallics* **1997**, *16*, 3737.

(11) Lukehart, C. M. *Fundamental Chemistry of Cyano Complexes of the Transition Metals*; Academic Press: London, 1976; p 77.

(12) (a) Jiang, J.; Koch, S. A. *Angew. Chem., Int. Ed.* **2001**, *40*, 2629.

(b) Carriedo, G. A.; Crespo, M. C.; Riera, V.; Sánchez, M. G.; Valin, M. L.; Moreiras, D.; Solans, X. *J. Organomet. Chem.* **1986**, *302*, 47.

(13) Tom Dieck, H.; Friedel, H. *J. Organomet. Chem.* **1968**, *14*, 375.

(14) In Figure 2b, obtained by spatial rotation of 2a, a ball-and-stick representation was used for clarity.

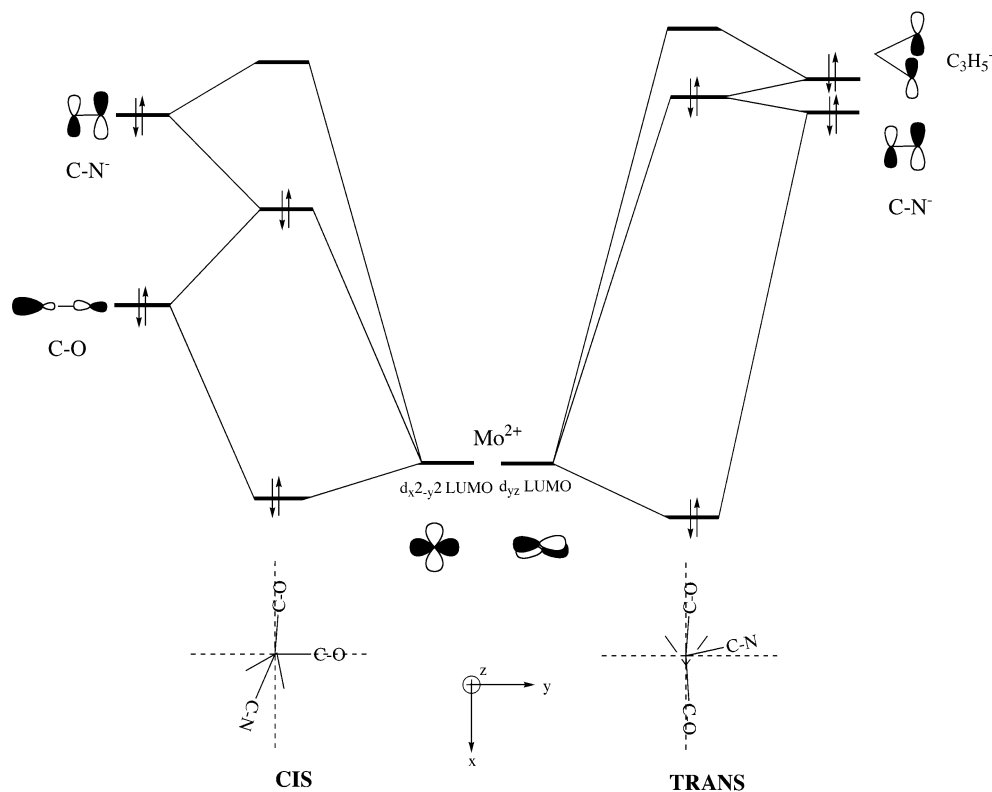


Figure 3. Main orbital interactions diagram for $[\text{Mo}(\text{CN})(\eta^3\text{-C}_3\text{H}_5)(\text{CO})_2(\text{dmpm})]$ (**3**).

Table 1. Crystal Data and Refinement Details for Complexes 2 and 3

	2	3
formula	$\text{C}_{10}\text{H}_{19}\text{MoN}_3\text{O}_2\text{P}_2$	$\text{C}_{11}\text{H}_{19}\text{MoNO}_2\text{P}_2$
fw	371.16	353.16
cryst syst	monoclinic	monoclinic
space group	$P2(1)/n$	$P2(1)/n$
<i>a</i> , Å	7.723(2)	8.706(5)
<i>b</i> , Å	14.189(3)	13.546(5)
<i>c</i> , Å	14.656(6)	14.246(5)
α , deg	90	90
β , deg	101.20(3)	101.17(5)
γ , deg	90	90
<i>V</i> , Å ³	1575.5(9)	1648.2(13)
<i>Z</i>	4	4
<i>T</i> , K	293(2)	293(2)
<i>D_c</i> , g cm ⁻³	1.565	1.423
<i>F</i> (000)	752	716
$\lambda(\text{Mo K}\alpha)$, Å	0.71073	0.71073
cryst size, mm	$0.50 \times 0.25 \times 0.1$	$0.20 \times 0.20 \times 0.03$
μ , mm ⁻¹	1.033	8.254
scan range, deg	$2.02 \leq \theta \leq 25.97$	$4.55 \leq \theta \leq 66.47$
abs corr	SADABS	SADABS
no. of reflns measd	3210	2494
no. of ind reflns	3089	2494
no. of data/restraints/params	3089/0/224	2494/0/173
goodness-of-fit on <i>F</i> ²	1.052	1.005
<i>R</i> ₁ / <i>R</i> _{w2} [<i>I</i> > 2σ(<i>I</i>)]	0.0290/0.0730	0.00802/0.1988
<i>R</i> ₁ / <i>R</i> _{w2} (all data)	0.0524/0.0839	0.0920/0.2035

thus making the two CO ligands and the halves of the allyl group inequivalent, as indicated by the ¹H and ¹³C spectra. This allyl orientation can be rationalized using simple MO arguments.¹⁵ Figure 3 displays the main interactions between the fragment $\{\text{Mo}(\text{CN})(\text{CO})_2(\text{dmpm})\}$ and the allyl ligand. Metal orbitals were derived from $d^4\text{-ML}_5$ FMOs¹⁶ by considering the presence of two mutually *trans* CO groups and one CN⁻

ligand. The strongest bonding combination was that of the π_2 allyl MO with the LUMO of the metal fragment. Additionally, a minor stabilization was produced due to the back-donation from the d_{xy} metal orbital to the π_3 allyl antibonding combination. The maximum overlap between these FMOs was attained when the relative orientation of the allyl ligand and the OC–Mo–CO vector is the one found in **3**.

Whereas this simple picture seems appropriate to rationalize the allyl orientation in **3**, we have performed DFT calculations in an attempt to obtain information on the factors governing the different structures found for **2** and **3**.

B3LYP calculations using the LANL2DZ and LANL1DZ basis sets for Mo and P atoms, respectively, and the 3-21G basis set for C, N, O, and H atoms render the *trans* isomer of $[\text{Mo}(\text{CN})(\eta^3\text{-C}_3\text{H}_5)(\text{CO})_2(\text{dmpm})]$ (with a rotational allyl orientation qualitatively in agreement with the previously mentioned EHMO arguments) 3.01 kcal/mol more stable than the *cis* one in Gibbs energy in solution.¹⁷ Parallel calculations showed *cis*- $[\text{Mo}(\text{N}_3)(\eta^3\text{-C}_3\text{H}_5)(\text{CO})_2(\text{dmpm})]$ to be 0.45 kcal/mol more stable than the *trans* isomer. Optimized geom-

(16) Albright, T. A.; Burdett, J. K.; Whangbo, M. H. *Orbital Interactions in Chemistry*; Wiley: New York, 1985.

(17) Calculations were performed with the Gaussian 98 series of programs including the effect of dichloromethane as solvent by means of the PCM method ($\epsilon = 8.93$): Montgomery, J. A., Jr.; Stratmann, R. E.; Burant, J. C.; Dapprich, S.; Millam, J. M.; Daniels, A. D.; Kudin, K. N.; Strain, M. C.; Farkas, O.; Tomasi, J.; Barone, V.; Cossi, M.; Cammi, R.; Mennucci, B.; Pomelli, C.; Adamo, C.; Clifford, S.; Ochterski, J.; Petersson, G. A.; Ayala, P. Y.; Cui, Q.; Morokuma, K.; Malick, D. K.; Rabuck, A. D.; Raghavachari, K.; Foresman, J. B.; Cioslowski, J.; Ortiz, J. V.; Stefanov, B. B.; Liu, G.; Liashenko, A.; Piskorz, P.; Komaromi, I.; Gomperts, R.; Martin, R. L.; Fox, D. J.; Keith, T.; Al-Laham, M. A.; Peng, C. Y.; Nanayakkara, A.; Gonzalez, C.; Challacombe, M.; Gill, P. M. W.; Johnson, B.; Chen, W.; Wong, M. W.; Andres, J. L.; Gonzalez, C.; Head-Gordon, M.; Replogle, E. S.; Pople, J. A. *Gaussian 98*; Gaussian, Inc.: Pittsburgh, PA, 1998.

(15) EH calculations have been carried out with the model *trans*- $[\text{Mo}(\text{CN})(\text{C}_3\text{H}_5)(\text{CO})_2(\text{PH}_3)_2]$. Details available from Prof. A. Galindo (galindo@us.es).

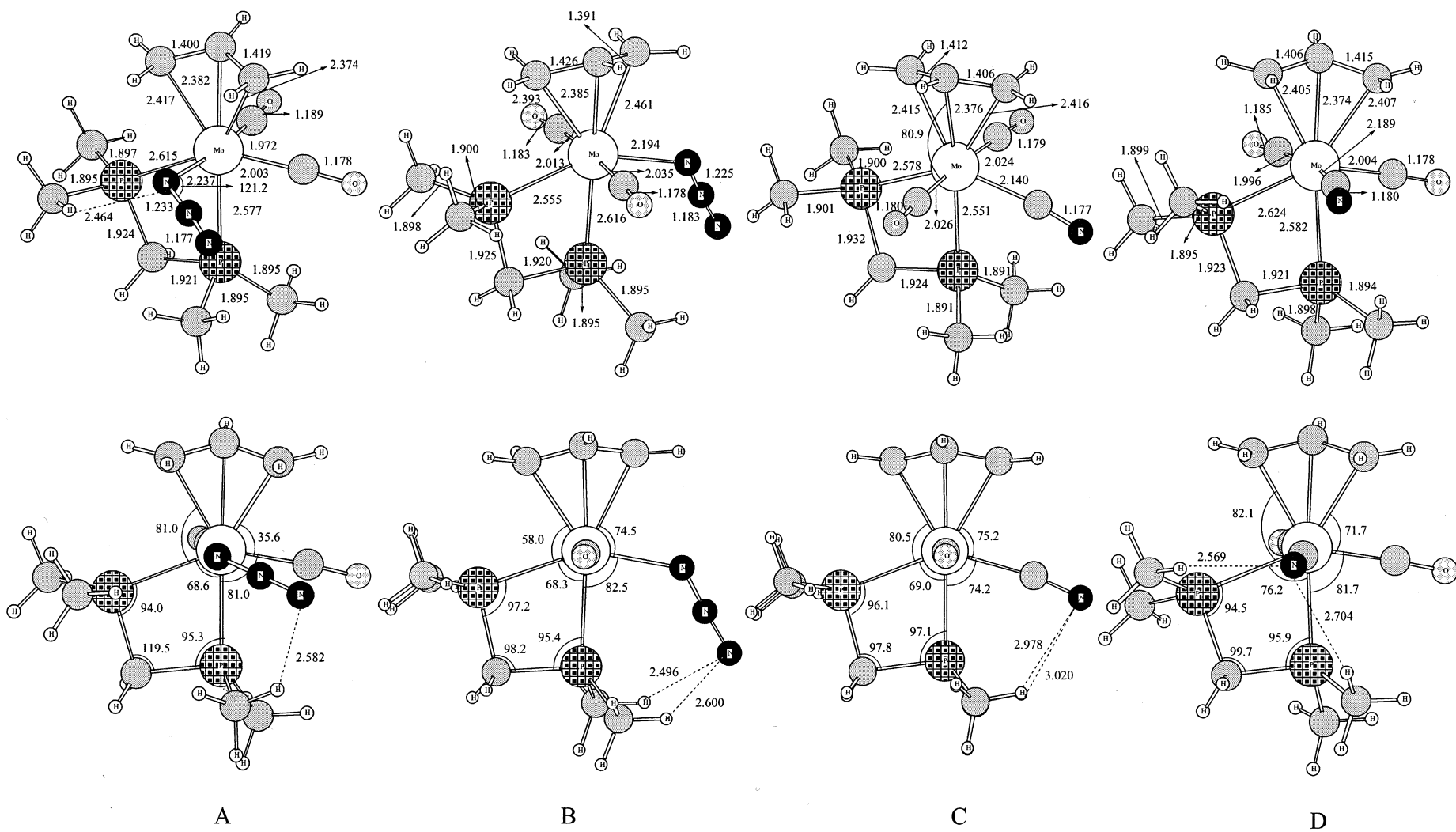
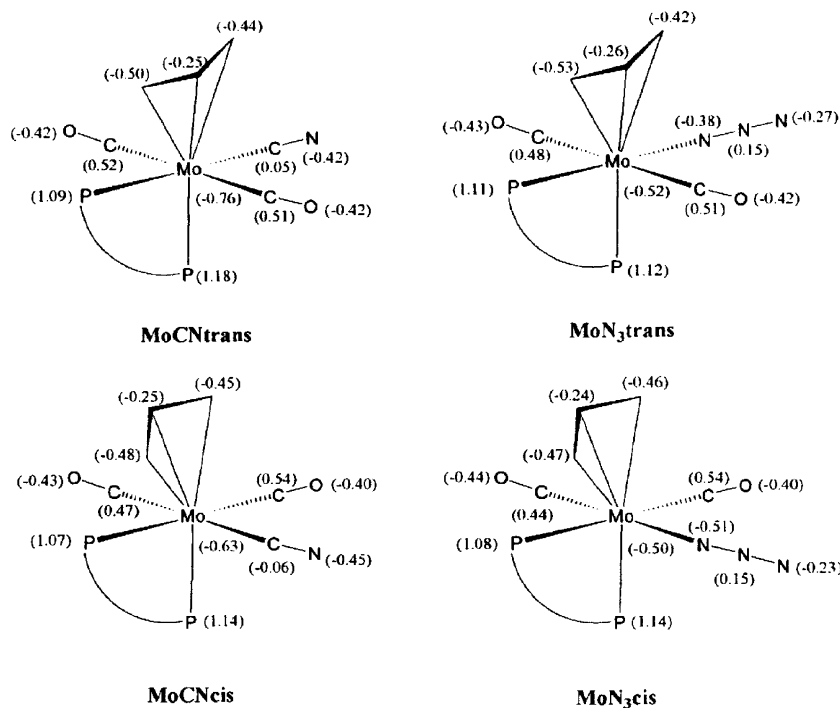


Figure 4. Optimized geometries of (A) *trans*-[Mo(N₃)(η^3 -C₃H₅)(CO)₂(dmpm)], (B) *cis*-[Mo(N₃)(η^3 -C₃H₅)(CO)₂(dmpm)], (C) *trans*-[Mo(CN)(η^3 -C₃H₅)(CO)₂(dmpm)], and (D) *cis*-[Mo(CN)(η^3 -C₃H₅)(CO)₂(dmpm)].

Table 2. B3LYP Calculations for **2** and **3** Using the LANL2DZ and LANL1DZ Basis Sets for Mo and P Atoms, Respectively, and the 3-21G Basis Set for C, N, O, and H Atoms^a

isomer	ΔE_0	ΔE_{ZPVE}	ΔH	$-T\Delta S$	$\Delta G_{\text{gas-phase}}$	$\Delta\Delta G_{\text{solvation}}$	$\Delta G_{\text{solvation}}$
[Mo(CN)(η^3 -C ₃ H ₅)(CO) ₂ (dmpm)] (3)							
<i>trans</i>	0.00	0.00	0.00	0.00	0.00	0.0	0.00
<i>cis</i>	1.63	0.36	1.86	0.47	2.33	0.68	3.01
[Mo(N ₃)(η^3 -C ₃ H ₅)(CO) ₂ (dmpm)] (2)							
<i>cis</i>	0.00	0.00	0.00	0.00	0.00	0.00	0.00
<i>trans</i>	1.61	-0.16	1.43	0.14	1.57	-1.12	0.45

^a The effect of dichloromethane as solvent was included by the PCM method ($\epsilon = 8.93$). Energies in kcal/mol.

**Figure 5.** Net natural population analysis charges for **2** and **3**.

erties and energies are given in Figure 4 and Table 2, and the results of the net natural population analysis charges are summarized in Figure 5. The NPA charge¹⁸ on the metal atom of **3** is -0.63 in the *cis* isomer and -0.76 in the *trans* one. The NPA charges on all the ligands are similar in both isomers except for CN⁻, which presents a net charge of -0.51 and -0.37 in the *cis* and *trans* structures, respectively.

An analysis of the Kohn–Sham MOs of [Mo(CN)(η^3 -C₃H₅)(CO)₂(dmpm)] (**3**) in terms of those of the metal atom and the ligands¹⁹ shows that the most important fragment electronic configurations describing the *trans* structure imply electron transfers from the HOMOs of C₃H₅⁻ and CN⁻ to the LUMO of Mo²⁺. In contrast, in the *cis* isomer the relative weight of these electronic configurations considerably diminish, the electron transfers from the HOMOs of the CO ligands to the LUMO of Mo²⁺ becoming dominant, particularly those configurations corresponding to back-donation from the metal to the CO's.

The above-mentioned differences in energy and electronic structure between the *cis* and *trans* isomers of [Mo(CN)(η^3 -C₃H₅)(CO)₂(dmpm)] can be easily rational-

ized taking into account the main interactions between CN and the metal atom. As displayed by the diagram in Figure 3, our analysis reveals that, in the *trans* isomer, the HOMOs of CN⁻ and C₃H₅⁻ interact mainly with the d_{yz} LUMO of the metal, whereas in the *cis* isomer the HOMO of CN⁻ and the HOMO of one of the CO ligands present the most important interaction with the d_{x²-y²} LUMO of Mo²⁺. From the diagram it is clear that this different interaction pattern can explain the fact that CN⁻ behaves as a better electron donor in the *trans* structure and appears to determine the preferential stabilization of that isomer.

Therefore, our theoretical analysis establishes the strong σ -donor character of the cyano ligand as responsible for the encountered difference between the structures of **2** and **3**.²⁰

Experimental Section

All manipulations were carried out under nitrogen using standard Schlenk techniques. Solvents were distilled from Na (hexane), NaOMe (MeOH), and CaH₂ (CH₂Cl₂). CD₂Cl₂ was dried over molecular sieves (4 Å) and stored over Na₂CO₃ in Young tubes in the dark. Elemental analyses were obtained using a Perkin-Elmer 240-B microanalyzer. The IR and NMR spectra were recorded on Perkin-Elmer FT 1720-X (over the

(18) Weinhold, F.; Carpenter, J. E. *The Structure of Small Molecules and Ions*; Plenum: New York, 1988.

(19) This analysis was performed by using the ANACAL program: López, R.; Menéndez, M. I.; Suárez, D.; Sordo, T. L.; Sordo, J. A. *Comput. Phys. Commun.* **1993**, *76*, 235–249.

(20) Dunbar, K. R.; Heintz, R. A. *Prog. Inorg. Chem.* **1997**, *45*, 283.

range 2200–1600 cm^{-1}) and Bruker AC-200 (or AC-300) spectrometers, respectively, using TMS as internal reference.

Synthesis of 1. Under N_2 , dmpm (56 μL , 0.35 mmol) was added to a solution of $[\text{MoCl}(\eta^3\text{-C}_3\text{H}_5)(\text{CO})_2(\text{NCMe})_2]^{13}$ (0.110 g, 0.35 mmol) in CH_2Cl_2 (10 mL). After 5 min stirring the volume was reduced in vacuo to 5 mL and hexane (20 mL) was layered, giving (2 days at -20°C) red crystals of **1**. Yield: 0.120 g, 93%. Anal. Calcd for $\text{C}_{10}\text{H}_{19}\text{ClMoO}_2\text{P}_2$: C, 32.94; H, 5.25. Found: C, 33.21; H, 4.97. IR (CH_2Cl_2): 1944(s), 1845(s) cm^{-1} . $^{31}\text{P}\{^1\text{H}\}$ NMR (CD_2Cl_2): δ -24.38. ^1H NMR (CD_2Cl_2): δ 4.75(m, 1H, H_c); 3.69(m, 2H, H_{syn}); 3.24(m, 2H, CH_2 dmpm); 2.31(d, $^3J(\text{H,H}) = 11.7$, 2H, H_{anti}); 1.73(t, $^2J(\text{P,H}) = 4.8$, 6H, CH_3 dmpm); 1.65(t, $^2J(\text{P,H}) = 5.2$, 6H, CH_3 dmpm). $^{13}\text{C}\{^1\text{H}\}$ NMR (CD_2Cl_2): 226.68(t, $^2J(\text{P,C}) = 7.6$, CO); 98.68(s, C_2 allyl); 62.36(s, C_1 and C_3 allyl); 40.65(t, $^1J(\text{P,C}) = 23.2$, CH_2 dmpm); 17.34(t, $^1J(\text{P,C}) = 13.6$, CH_3 dmpm); 13.40(t, $^1J(\text{P,C}) = 12.8$, CH_3 dmpm).

Synthesis of 2. Sodium azide (0.017 g, 0.27 mmol) was added to a solution of **1** (0.100 g, 0.27 mmol) in 15 mL of a mixture of $\text{CH}_2\text{Cl}_2/\text{MeOH}$ (5:1, v/v). Stirring (90 min), solvent evaporation in vacuo, extraction of the residue (CH_2Cl_2 , 10 mL), filtration (Celite), in vacuo concentration (to 5 mL), and layering with hexane (20 mL) afforded, after 2 days at -20°C , orange crystals. Yield: 0.01 g, 68.7%. Anal. Calcd for $\text{C}_{10}\text{H}_{19}\text{MoN}_3\text{O}_2\text{P}_2$: C, 32.36; H, 5.16; N, 11.32. Found: C, 32.56; H, 5.34; N, 11.12. IR (CH_2Cl_2): 2072(s), 1936(s), and 1851(s) cm^{-1} . $^{31}\text{P}\{^1\text{H}\}$ NMR (CD_2Cl_2): δ -22.38, s. ^1H NMR (CD_2Cl_2): δ 4.82(m, 1H, H_c); 3.70(m, 2H, H_{syn}); 3.28(at, $^2J(\text{H,P}) = 10$, 2H, CH_2 dmpm); 2.19(d, $^3J(\text{H,H}) = 12$, 2H, H_{anti}); 1.71(m, 12H, CH_3 dmpm). $^{13}\text{C}\{^1\text{H}\}$ NMR (CD_2Cl_2): 226.51(at, $^2J(\text{P,C}) = 8$, CO); 62.30(s, C_1 allyl); 57.86(s, C_2 allyl); 40.93(at, $J(\text{P,C}) = 24$, CH_2 dmpm); 17.56(at, $J(\text{P,C}) = 15$, CH_3 dmpm); 16.43(d, $J(\text{P,C}) = 23$, CH_3 dmpm); 14.62(at, $J(\text{P,C}) = 11$, CH_3 dmpm).

Synthesis of 3. Sodium cyanide (0.016 g, 0.32 mmol) was added to a solution of **1** (0.100 g, 0.32 mmol) in 15 mL of a mixture of $\text{CH}_2\text{Cl}_2/\text{MeOH}$ (5:1, v/v). After 6 h stirring, workup as for **2** gave **3** as a pale yellow powder. Yellow crystals of **3** were obtained by slow diffusion of hexane into a concentrated solution of **3** in CH_2Cl_2 at -20°C . Yield: 0.078 g, 68.4%. Anal. Calcd for $\text{C}_{11}\text{H}_{19}\text{MoNO}_2\text{P}_2$: C, 37.20; H, 5.39; N, 3.94. Found: C, 37.47; H, 5.12; N, 3.72. IR (CH_2Cl_2): 2096(w), 1867(vs) cm^{-1} . $^{31}\text{P}\{^1\text{H}\}$ NMR (CD_2Cl_2): δ -11.4, -21.4 (ABq, $^2J(\text{P,P}) = 85.4$). ^1H NMR (CD_2Cl_2): δ 5.21(m, 1H, H_c); 3.20(m, 2H, CH_2 dmpm); 3.08(dd, $^3J(\text{P,H}) = 7.0$, $^2J(\text{H,H}) = 3.2$, 1H, H_{syn}); 2.77(d, $^3J(\text{H,H}) = 12.2$, 1H, H_{anti}); 2.21(m, 2H, H_{anti} , H_{syn}); 1.96(d, $^2J(\text{P,H}) = 9.8$, 3H, CH_3 dmpm); 1.73(t, $^2J(\text{P,H}) = 9.9$, 6H, CH_3 dmpm); 1.59(d, $^2J(\text{P,H}) = 9.1$, 3H, CH_3 dmpm). $^{13}\text{C}\{^1\text{H}\}$ NMR (CD_2Cl_2): 211.53(t, $^2J(\text{P,C}) = 10.1$, CO); 209.33(t, $^2J(\text{P,C}) = 8.3$, CO); 145.81(d, $^2J(\text{P,C}) = 17.1$, CN); 98.67(s, C_2 allyl); 53.96(s, C_1 allyl); 45.47(d, $^2J(\text{P,C}) = 9.2$, C_3 allyl); 40.88(t, $^1J(\text{P,C}) = 24$, CH_2 dmpm); 20.35(t, $^1J(\text{P,C}) = 3.2$, CH_3 dmpm); 18.50(t, $^1J(\text{P,C}) = 6.0$, CH_3 dmpm).

Acknowledgment. We thank the Ministerio de Ciencia y Tecnología (grants BQU2000-0220 and BQU2000-0219) and Principado de Asturias (grants PR-01-GE-7 and PR-01-GE-4) for support of this work.

Supporting Information Available: Tables giving positional and thermal parameters, bond distances and bond angles for **2** and **3**. This material is available free of charge via the Internet at <http://pubs.acs.org>.

OM020919M